

Exploring lipophilic antioxidants accumulation in field-grown low temperature-stressed *Ephedra monosperma*

V.E. SOFRONOVA^{1,*} , V.V. NOKHSOROV¹ , F.F. PROTOPOPOV² , B. NOWICKA³ ,
M. JEMIOŁA-RZEMINSKA³ , and K. STRZALKA^{3,4} 

¹Institute for Biological Problems of Cryolithozone, Siberian Branch, Russian Academy of Sciences, Yakutsk, 677000, Russia

²Institute of Physics and Technologies, North-Eastern Federal University, Yakutsk, 677000, Russia

³Department of Plant Physiology and Biochemistry, Faculty of Biochemistry, Biophysics and Biotechnology, Jagiellonian University, Krakow, 30-387, Poland

⁴Malopolska Centre of Biotechnology, Jagiellonian University, Krakow, 30-387, Poland

*Corresponding author: E-mail: vse07_53@mail.ru

Abstract

The seasonal patterns of changes in the content of lipophilic antioxidants β -carotene (β -Car), zeaxanthin (Zx), α -tocopherol (α -Toc), plastoquinone (PQ)/plastoquinol (PQH₂) were studied in the assimilating shoots of evergreen shrub *Ephedra monosperma* J.G. Gmel ex C.A. Mey under natural conditions of Central Yakutia. The shortening of the photoperiod and the seasonal decrease in temperature induced a 1.4-fold increase in α -Toc content. The fall in the average daily temperature from 0.1 to -8.1°C in October led to a decrease in the content of β -Car as a result of the accumulation of rhodoxanthin (Rhd). In this period a sharp increase in the content of Zx retained overnight was also detected. In winter, elevated content of Zx and α -Toc persisted. During September, the content of PQH₂ increased by 2.5 times and PQ by 1.4 times (compared to July). The beginning of exposure to freezing average daily temperatures from -3 to -5°C led to the depletion of the total PQ pool by 18%. However, the content of PQ_{tot} in the winter months was 1.5 times higher than at the end of July. The results revealed different timing and temperature ranges of variation for individual antioxidants during the development of frost resistance in ephedra.

Keywords: *Ephedra monosperma*, low temperatures, low-molecular-mass lipophilic antioxidants, OJIP fluorescence induction curve.

Introduction

Extremely low in winter (up to -50°C) and very high in summer (up to 35°C) temperatures characterize the sharp continental climate of Central Yakutia. This territory is located in the permafrost zone (Zhirkov *et al.* 2021). Under the conditions of strict climate and permafrost edaphic control evergreen tree species (pine, spruce) do

not form large forests. The share of evergreen forests is approximately 10% of the forest cover. In contrast, evergreen shrubs (especially *Vaccinium vitis-idaea*, *Arctostaphylos uva-ursi*, *Ledum palustre*), overwintering under snow cover, are ubiquitous.

Central Yakutia is characterized by a rapid autumnal decrease in temperature. The temperature reduction proceeds steeper than the shortening of photoperiod as

Received 15 February 2023, last revision 5 September 2023, accepted 3 October 2023.

Abbreviations: Ax - antheraxanthin; β -Car - β -carotene; ¹Chl* - singlet excited state of chlorophyll; F_m - maximal fluorescence yield; F₀ - minimal fluorescence yield; NPQ - nonphotochemical quenching of chlorophyll fluorescence; ¹O₂* - singlet oxygen; OJIP curve - Chl *a* fluorescence transient; PGs - plastoglobules; PQ - plastoquinone; PQH₂ - plastoquinol; PQ_{tot} - total level of PQ (oxidized plus reduced); PSII - photosystem II; Q_A - primary quinone acceptor of electrons in PSII; RCs - reaction centers; Rhd - keto-carotenoid rhodoxanthin; α -Toc - α -tocopherol; V_J - relative variable fluorescence at the J-step; Vx - violaxanthin; Zx - zeaxanthin; ϕ_{P_0} - quantum yield for electron transport; ϕ_{P_0} - maximum quantum yield for primary photochemistry.

Acknowledgements: This work was funded by the Russian Science Foundation (project No. 22-76-00043). Field work was carried out in the framework of the State Task of the Ministry of Education and Science of the Russian Federation FWRS-2021-0024.

Conflict of interest: The authors declare that they have no conflict of interest.

compared to the gradients of the above parameters in geographical regions with a milder climate at the same latitude. Cold adaptation lasts in Central Yakutia for approximately six to seven weeks, from the beginning of September to mid-October. The seasonal decrease in the average daily temperature from 10 to 12°C to the freezing levels of -3 to -8°C and the reduction of the photoperiod from 14 to 10 h in this time frame convert evergreen plants to their winter-acclimated condition in which they are able to tolerate extremely low winter temperatures (range from -30 to -50°C).

Low temperatures can lead to oxidative stress. Plants counteract photo-oxidative damage by fine-tuning a variety of photoprotective and antioxidant mechanisms based on specialized metabolites that keep reactive oxygen species (ROS) at a concentration efficient for signalling (Fernández-Marín *et al.* 2017). In particular, these mechanisms are associated with the plasticity of chlorophyll content, and low-molecular-mass non-enzymatic lipophilic antioxidants such as α -Toc, β -Car, and Zx.

Retro-red carotenoids (most often Rhd) have been reported in some evergreen plants (*Thuja plicata*, *Cryptomeria japonica*, *Thuja occidentalis*) during winter (Maslova *et al.* 2009, Katahata *et al.* 2021). To the best of our knowledge, the photoprotective function of *retro*-carotenoids remains controversial. The first is based on the fact that Rhd serves as an effective broad-band internal trap for radiation in the green range, aimed at decreasing the amount of radiation absorbed by photosynthetic apparatus (Merzlyak *et al.* 2005). However, the presence of red (*retro*-carotenoids (eschschooltzanthin and its derivatives) in the upper mesophyll of *Buxus sempervirens* leaves did not change the extent of photoinhibition (Hormaeche *et al.* 2005). Although reported results are not always consistent, the photoprotective function of *retro*-carotenoids in evergreen plants remains the leading hypothesis for explanation of adaptive winter reversible reddening.

Although plants have the same set of low-molecular-mass lipophilic antioxidants (α -Toc, β -Car, and Zx), significant differences of their content have been identified depending on taxonomy, growth stage, and also in response to stressful conditions (Fernández-Marín *et al.* 2017). Seasonal changes in lipophilic antioxidants represent a common phenomenon. Despite a sufficient number of studies on the variability of lipophilic antioxidants in response to low temperatures in late autumn and winter in woody evergreens (García-Plazaola *et al.* 2003, González-Rodríguez *et al.* 2019) such studies have not yet been carried out in evergreens growing in Central Yakutia.

Ephedra monosperma is a relict evergreen coniferous dwarf shrub that has survived from the pre-glacial period. The natural area of this species covers Siberia and the Russian Far East. *E. monosperma* is a sun-loving and drought-tolerant plant species. Assimilation is carried out by numerous branched green shoots. They are long-lived and are subjected to a succession of different stress conditions during their lifespan. Green shoots show winter reddening, coinciding with the accumulation of Rhd

before winter (Sofronova *et al.* 2014). The red-brown shoots turn green again when photosynthesis resumes in late spring. The extreme tolerance of *E. monosperma* to harsh environments makes it invaluable for exploring photoprotective and cold tolerance mechanisms.

The study was aimed at characterizing the changes in lipophilic antioxidants (α -Toc, β -Car, Zx, PQ/PQH₂) in response to low-temperature stress during the autumn-winter period in ephedra plants. Our experiments covered all principal stages of woody plant cold hardening: the transition to dormancy that progressed to first stage of hardening (at temperatures from 10 to 0°C) and then to second stage (at temperatures from 0 to -10°C) as well as the winter dormancy. We wanted to check if the acclimation of *E. monosperma* to freezing stress is accompanied by the increase in the content of certain prenolipid protective compounds belonging to xanthophylls and isoprenoid quinones and chromanols.

Materials and methods

Study site description and sample collection: *Ephedra monosperma* J.G. Gmel. ex C.A. Mey plants grow naturally in the botanical garden of the Institute for Biological Problems of Cryolithozone, Siberian Branch, Russian Academy of Sciences. The garden area is located on the second terrace above the flood plain of the Lena valley (62°15'N, 129°37'E). The air temperature on the experimental plot was recorded at 1-h intervals using a DS 1922L iButton thermograph (Dallas Semiconductor, Dallas, USA). Irradiance was measured with a LI-190 sensor (LI-COR, Lincoln, NE, USA). The daily incidence of solar radiation was determined by averaging data recorded at half-hour intervals from dawn to sunset and was expressed in $\mu\text{mol}(\text{photon})\text{m}^{-2}\text{s}^{-1}$.

For the analysis of chlorophylls (Chls), carotenoids, α -Toc, and PQ/PQH₂ the samples were collected 8 times from 31 July 2019 to 21 January 2020. The current year shoots were cut into 4 to 5 cm segments prior to sunrise and immediately transported to the laboratory in a thermostatic bag at natural air temperature. Then, they were quickly fixed in liquid nitrogen and desiccated in a VirTis lyophilizer (New York, NY, USA). Lyophilizates were stored at -80°C.

Sample extraction and quantification of pigments: For each extraction, to 20 mg of dry plant material 1.5 ml of chloroform:methanol (2:1, v/v) mixture was added and the sample was shaken for 1 h. Next, the samples were centrifuged (5 min, 9 000 g). The supernatant was collected. The pellet was not colorless, which means that not all pigments were extracted. Therefore, the pellet was ground in a mortar with 2 ml of chloroform:methanol (2:1, v/v) mixture. After grinding, the suspension was centrifuged (5 min, 9 000 g), resulting in a green supernatant and a colorless pellet. This supernatant was combined with the supernatant obtained earlier. The combined extracts were evaporated using gaseous nitrogen and stored at -20°C.

The concentrations of Chls and total carotenoids were determined spectrophotometrically. The evaporated samples were resuspended in 1.5 ml of methanol. The samples were diluted 5 times. Then the absorption of the diluted samples was measured for $\lambda = 665.2$, 652.4 , and 470 nm. Pigment content was calculated according to Lichtenthaler (1987).

Determination of β -Car, Zx, Vx, and Ax by HPLC:

21 - 24 mg of dry plant material were dissolved in 1 ml of extraction medium [methanol, 0.2 M ammonium acetate, ethyl acetate (81:9:10, v/v)], shaken for 10 min and centrifuged (3 min, 9 000 g). The supernatant was collected, and extraction was repeated. After combining of the supernatants 1 ml was taken and filtered using Millex-GN syringe filter Nylon, pore size 0.2 μm (Merck KGaA, Darmstadt, Germany).

20 μl of pigment extract was injected into 0.5 ml of extraction medium and analyzed on a Nucleosil Column (ET 250/8/4, 300-5, C₁₈; Macherey-Nagel, Düren, Germany) by HPLC. The elution was carried out using solvent A (methanol, 0.5 M aqueous ammonium acetate, 85:15, v/v), solvent B (acetonitrile to water, 90:10, v/v) and solvent C (ethyl acetate) in a linear gradient (minutes/% solvent A/% solvent B/% solvent C): 0/60/40/0, 2/0/100/0, 7/0/80/20, 17/0/50/50, 21/0/30/70, 28.5/0/30/70, 29.5/0/100/0, 30.5/60/40/0, at a flow rate of 0.8 ml/min (Kuczynska and Jemiola-Rzeminska 2017).

Reversed-phase HPLC was performed on an Agilent 1200 Series HPLC system (Agilent Technologies, Santa Clara, California, USA) equipped with a photodiode array detector and controlled by Agilent ChemStation software. Pigments were identified by comparing the online spectra with data from the literature and quantified using calibration curves calculated with standards.

Rhodoxanthin extraction and assay: Rhd was twice extracted with chloroform:methanol (2:1, v/v) extraction mixture (EM) from fresh plant material (2.5 ml of EM per 250 mg of sample). After centrifugation (5 min, 9 000 g), the supernatants were combined. The extract was concentrated to a volume of 0.2 ml and purified by TLC (Sofronova et al. 2014). The content of Rhd was quantified by taking that its mass absorption coefficient A in chloroform is 2 500 at 507 nm (Merzlyak et al. 2005).

HPLC analysis of isoprenoid chromanols and quinones (α -Toc, PQ, and PQH₂):

For HPLC separation, evaporated samples were resuspended in 1.5 ml of methanol. HPLC analysis of both redox forms of plastoquinone was performed in the following system: Teknokroma (Barcelona, Spain) C₁₈ reverse phase column (Nucleosil 100, 250 \times 4 mm, 5 μm), eluent – methanol:hexane (340:20, v/v), flow rate of 1.5 ml/min, absorption detection at 255 nm, fluorescence detection at $\lambda_{\text{ex}} = 290$ nm, $\lambda_{\text{em}} = 330$ nm. Analysis of α -Toc, δ -Toc, γ -Toc and α -tocopherolquinone (α -TQ) was performed using HPLC: C₁₈ reverse phase column same as above and platinum postcolumn, eluent – methanol:water (95:5, v/v), flow rate of 1 ml/min, fluorescence detection as described

above. Platinum postcolumn (5% on alumina, powder, 325 mesh, Sigma-Aldrich) was needed for the reduction of α -tocopherolquinone to α -tocopheryloquinol, which can be easily detected by fluorescence measurements (Kruk and Trebst 2008, Nowicka and Kruk 2012).

Measurements of OJIP curves: The seasonal dynamics of the Chl fluorescence induction curves (OJIP) was monitored until September 25 under field conditions using a Pocket PEA portable fluorometer (Hansatech Instruments, King's Lynn, Norfolk, UK). Before measurements, the shoots were covered with clips for 30 min for dark adaptation at ambient temperature. Fluorescence was induced by saturating light of 3 000 $\mu\text{mol}(\text{photon}) \text{m}^{-2} \text{s}^{-1}$, and transient fluorescence for 1 s was recorded with time intervals increasing from 10 μs during the first 300 μs of the measurement up to 100 ms intervals for a time longer than 0.3 s. The JIP-test parameters used in this research are listed in Table 1 Suppl., in which formulas, equations, and definitions are given according to Chen et al. (2014).

In experiments carried out on October 30 and December 12 at freezing temperatures, the assimilating shrub shoots with the root system excised before noon were immediately transported to the laboratory (~30 min) in a light proof thermostatic bag balanced to ambient temperature. Plant samples wrapped in wet towels, were transferred to a climatic chamber KBWF 720 (Binder, Germany), where they were kept in the dark for 20 min at 4°C and relative air humidity 50%. The current year shoots then were cut off and placed in leaf clips for 30 min on wet paper at 17°C in a climatic chamber. The measurements of the Chl *a* fluorescence transient (OJIP) of dark-adapted samples were carried out at 17°C. Each induction curve of Chl fluorescence (OJIP) for a given date was obtained by averaging of at least eight biological replicates.

Statistical analysis: The experiments were performed with at least three biological replicates ($n = 3$) with three technical repetitions. The obtained data are presented as mean values with standard deviation (SD). Data analysis was performed by one-way analysis of variance (ANOVA) using the STATISTICA v. 10 software package (StatSoft, Tulsa, OK, USA). The means were compared using Duncan's multiple range test. Differences were considered statistically significant at $P \leq 0.05$. Different letters are used in the figures and tables to indicate significant differences.

Results

Weather conditions during the study period: The experiments were carried out since July 2019 to January 2020 (Table 1). The average daily air temperature decreased during this period from 24 to 25°C to the range between -30 and -46°C (Fig. 1), and the duration of photoperiod shortened from 17.4 to 5.1 h. The average air temperature during the growing season (May to September) was 13°C, the total liquid precipitation amounted to 123 mm. The beginning of weak frosts was observed from the beginning of the second half of September, and persistent lowering of mean night temperature below

Table 1. Timing of developmental stages for *Ephedra monosperma* plants and changes in average daily air temperature during the experiments. Temperatures present averaged data for 24 h (day-night cycle) before sampling. Means \pm SDs. Photoperiod data are taken from the website <https://planetcalc.ru/300/>.

Date	Stages of development and cold hardening	Temperature [$^{\circ}$ C]	Photoperiod [h]
July 31	end of the phase of fructification	17.8 ± 1.5	17.4
August 15	bud setting, completion of active growth	13.4 ± 1.7	16.0
September 11	onset of stage 1 hardening	7.3 ± 0.9	13.4
September 24	stage 1 hardening	4.7 ± 1.5	12.1
September 30	onset of stage 2 hardening	-1.0 ± 0.9	11.5
October 7	stage 2 hardening	-0.2 ± 2.1	10.9
October 17	completion of stage 2 hardening	-10.9 ± 3.5	9.9
January 21	winter dormancy	-44.7 ± 0.5	6.6

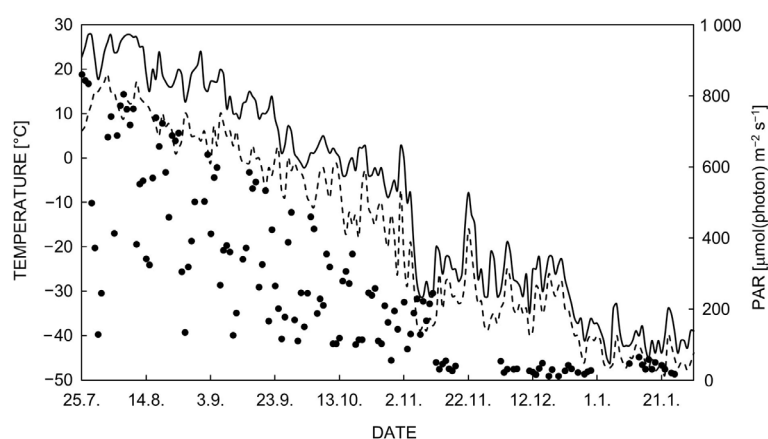


Fig. 1. Seasonal course of the maximum daily air temperature (*solid line*) and the minimum daily air temperature (*dotted line*) during the study period (2019 - 2020). PAR values shown in *black dots*.

the 0° C occurred after September 30. The minimum air temperatures in winter were from -44 to -47° C. The snow cover was established on October 13. The thickness of the snow layer was 2-10 cm at the end of October, 15-21 cm in the middle of November, 18-26 cm in December, and 24-34 cm in January. Temperature at a depth of 10 cm from the snow cover surface varied from -15 to -24° C in December and January.

Carotenoids: Total carotenoid content varied in the range of 0.7 to 0.8 mg g^{-1} (DM). According to our data, until the average daily temperature dropped to $3.6 \pm 1.2^{\circ}$ C between September 18 and 24, the proportion of photosynthetic carotenoids (β -Car, Nx, Vx, Ax, Zx, and lutein) remained comparable to the summer months and was about 70% of the total carotenoid content. However, with the onset of average daily temperatures of 0 to -5° C in early October, their proportion decreased to 60%, due to Rhd biosynthesis, and subsequently did not change. The identification of other carotenoids was not included in the task of our study.

The shoots had content of β -Car comparable to this observed during summer months (Fig. 2A), when average daily temperatures dropped from 7.3 to 4.7° C in September (Table 1). The effect of near-zero temperatures with night

frosts of $-5.8 \pm 4.3^{\circ}$ C lasting from the end of September to October 7 resulted in β -Car content being 40% lower than in the temperature range from 8 to 4° C. The final stage of a significant decrease in content of β -Car occurred in November to January, when the average daily temperature fell from -27 to -45° C. In January, the content of β -Car in the shoots was 2.5 times lower than in July (Fig. 2A).

The appearance of Rhd (β -Car derivative) in the ephedra shoots was shown in September; subsequently, it accumulated rapidly at near-zero average daily temperatures, peaking in mid-October (Fig. 2A). Throughout the autumn-winter period, the Rhd content was maintained at a stable high level. This pigment was present in the shoots until the beginning of active growth (end of May - early June) and then disappeared.

A transient increase in Vx content was observed in the first half of September. It was followed by the fall to the summer values on September 24 (Fig. 2B). Subsequently, a pronounced decrease in its content was revealed from September 25 to October 7. The measurements also showed a significant accumulation of Ax and Zx in the samples collected before sunrise (Fig. 2B). During November - January, a slow drop in Vx content was observed. On the contrary, Zx accumulated by mid-October persisted in the winter months.

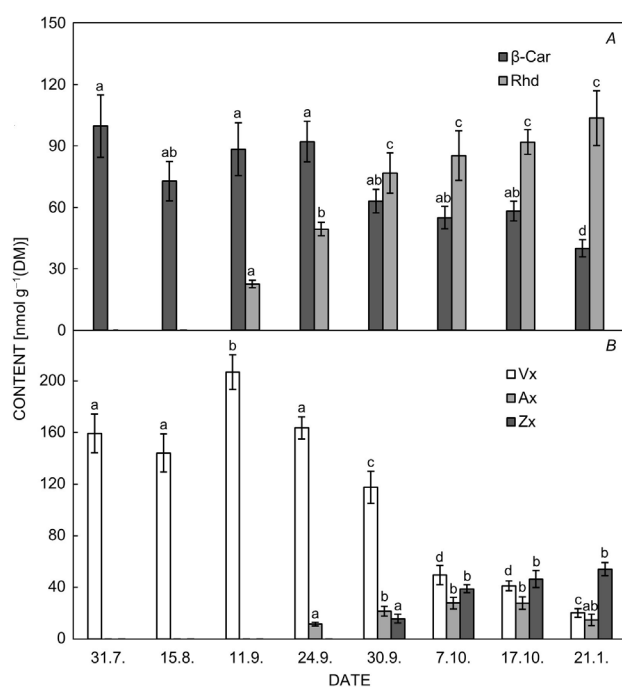


Fig. 2. Seasonal changes in the content of β -Car and Rhd (A), Vx, Ax, and Zx (B) at predawn during the study period in field-grown *E. monosperma*. Means \pm SDs, $n = 3$; different letters indicate significant differences ($P \leq 0.05$) between the dates of sampling.

Chlorophylls: In July - August the total chlorophyll (Chl) content varied in the range of 3.2 to 3.4 mg g⁻¹(DM). The onset of the decrease in Chl content was observed in August, when the cessation of vegetative plant growth was observed. The main decrease in Chl *a+b* content to 2.3 mg g⁻¹(DM) occurred during the period of cold hardening since the beginning of September until the end of the first decade of October. Severe winter negative temperatures from -15 to -47°C persisting in long-term induced a further decrease in total Chl by 13% in snow-covered plants. In January content of Chl *a+b* in the shoots was approximately 38 - 40% lower than in July due to their degradation.

α -Toc: The tocopherol composition in the assimilating shoots of *E. monosperma* was dominated by α -Toc, which accounted for more than 99% of total tocopherols. α -Toc content was lowest in July (Fig. 3A) and

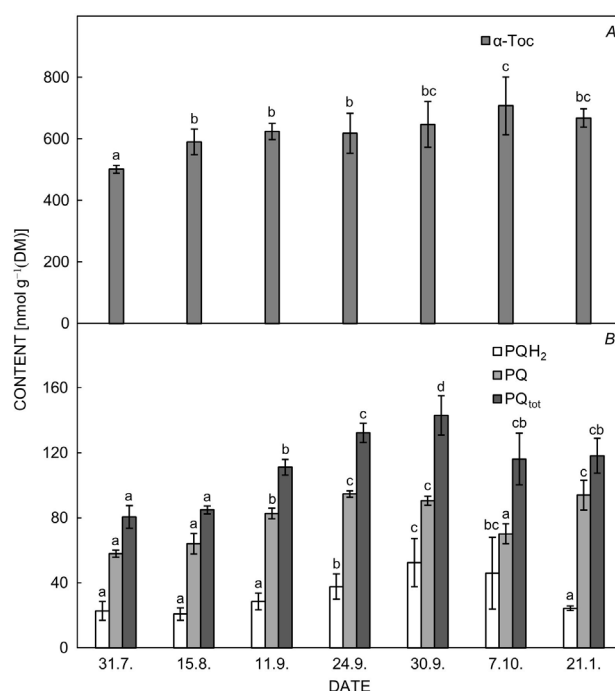


Fig. 3. Seasonal changes in the content of α -Toc (A), PQH₂, PQ, and PQ_{tot} (B) in the shoots of *E. monosperma*. Means \pm SDs, $n = 3$; different letters indicate significant differences ($P \leq 0.05$) between the dates of sampling.

progressively increased from mid-August to early October. The maximum values were detected on October 7, when there was a decrease of average daily temperatures to -5°C (Fig. 1). During the winter months, elevated content of α -Toc persisted. Its content was about 1.4 times higher than in July. However, it should be noted that the seasonal decrease in temperature caused an increase in the content of α -Toc only 1.2-fold compared to August (Table 2).

Plastoquinone/plastoquinol: In contrast to α -Toc, the dynamics of PQ_{tot} (oxidized plus reduced) in the assimilating shoots showed a pronounced dependence on low temperatures (Table 2). The content of PQH₂ since September 11 to the end of September increased 2.5-fold (compared to July), while that of PQ increased 1.4-fold. The content of PQ_{tot} increased nearly 1.7-fold (Fig. 3B). When plants were exposed to freezing temperatures of -2 to -5°C and average irradiance 250 - 460 μ mol(photon)

Table 2. Timing and temperature ranges of variability of lipophilic antioxidants for *Ephedra monosperma* plants during cold acclimation and the development of freezing resistance. Temperatures are given in average daily values. **Compared to August.

Antioxidant	Timing	Temperature range [°C]	Changes in content compared to July [%]
β -Car	from end of September to October 17	-1.0 to -8.1	-40
Zx (fraction unregulated by light)	from end of September to October 17	-1.0 to -8.1	appearance and increase to 35 nM g ⁻¹ (DM)
PQH ₂	during September	7.4 to -1.5	+150
PQ	during September	7.4 to -1.5	+40
α -Toc	from end of September to October 7	near zero	+20**

$\text{m}^{-2} \text{s}^{-1}$ at the beginning of October, a consumption of PQ and PQ_{tot} by 20% occurred, followed by a progressive decrease in content of PQH_2 to a value 2.2 times lower during the winter months. However, the content of PQ_{tot} remained constant from the beginning of October to the end of January and was 1.5-fold higher than in the summer months.

Changes in OJIP fluorescence kinetics: The OJIP curve recorded in July exhibited a typical OJIP shape (Fig. 4). Under normal temperature in August, the OJIP curve showed the onset of a mild decrease in F_0 , F_m , ϕ_{Po} , Ψ_o and an increase in V_j (Table 3). In September and early October at average daily temperatures decreasing from 7.6 to -1.5°C a remarkable change in the shape of the OJIP curves of the *Ephedra* shoots took place (Fig. 4). A gradual increase in relative variable fluorescence in the J-step (V_j) and a notable reduction of F_0 , F_m , ϕ_{Po} , ϕ_{Eo} were observed

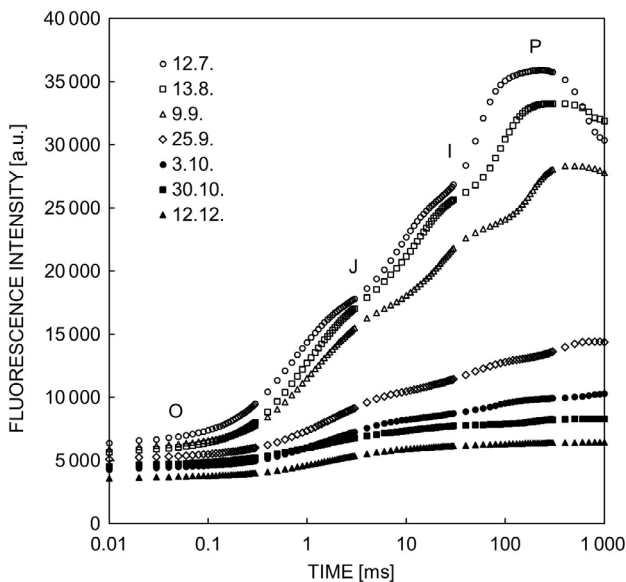


Fig. 4. Chlorophyll *a* fluorescence transient curves (OJIPs) in shoots of *E. monosperma* recorded on different dates. Each curve is the average of eight biological replicates. Mean temperatures for 24 h (day-night cycle) before measurements were 24.0, 15.7, 7.6, 3.5, -1.5 , -9.3 and -38.2°C , respectively, on the dates shown in the figure.

Table 3. Seasonal changes in JIP-test parameters in assimilating shoots of ephedra. Means \pm SDs ($n = 8$) and different letters indicate significant differences at $P \leq 0.05$ between the dates of sampling.

Date	$F_0 \times 10^{-3}$ [a.u.]	$F_m \times 10^{-3}$ [a.u.]	V_j	Ψ_o	ϕ_{Po}	ϕ_{Eo}
12.7.	6.90 ± 0.25^a	35.92 ± 2.09^a	0.38 ± 0.02^a	0.62 ± 0.02^a	0.81 ± 0.01^a	0.50 ± 0.02^a
13.8.	6.06 ± 0.36^b	33.28 ± 2.68^a	0.44 ± 0.03^b	0.56 ± 0.03^b	0.82 ± 0.02^a	0.46 ± 0.03^b
9.9.	6.31 ± 0.32^b	28.35 ± 2.83^b	0.45 ± 0.02^b	0.55 ± 0.02^b	0.78 ± 0.02^b	0.43 ± 0.03^c
25.9.	5.38 ± 0.34^c	14.44 ± 2.60^c	0.55 ± 0.02^c	0.45 ± 0.02^c	0.63 ± 0.05^c	0.29 ± 0.03^d
3.10.	4.49 ± 0.44^d	10.32 ± 2.03^d	0.61 ± 0.06^d	0.39 ± 0.06^d	0.56 ± 0.05^d	0.22 ± 0.03^c
30.10.	4.77 ± 0.41^d	8.32 ± 1.23^c	0.62 ± 0.02^d	0.38 ± 0.02^d	0.43 ± 0.07^c	0.16 ± 0.03^f
12.12.	3.73 ± 0.68^e	6.46 ± 1.57^f	0.76 ± 0.07^c	0.24 ± 0.07^c	0.42 ± 0.07^c	0.10 ± 0.03^g

(Table 3). The J-step became the dominant step of the fluorescence kinetics OJIP. At freezing temperatures from -9.3 to -38.2°C , in plants overwintering under snow cover, the values of F_0 , F_m , ϕ_{Po} continued to decrease, but to a lesser extent than during cold acclimation. In this period pronounced changes were revealed for V_j , Ψ_o , ϕ_{Eo} .

Discussion

The decrease in total Chl content from 3.43 to 2.13 $\text{mg g}^{-1}(\text{DM})$ during the study period can be attributed to the decay of antenna Chl-binding proteins and the dismantling of photosynthetic machinery (Verhoeven 2014). In thylakoid membranes, part of $\beta\text{-Car}$ is bound to the reaction center (RC) subunits and the core antennae in both photosystem (PS) I and PSII where it has a crucial photoprotective function, *i.e.*, quenching of the triplet excited state of Chl and scavenging of $^1\text{O}_2^*$ (Cazzaniga *et al.* 2012). It is worth mentioning that, in addition to thylakoids, outer and inner chloroplast envelope membranes, and plastoglobules (PGs) of chromoplasts also contain $\beta\text{-Car}$ (Royer *et al.* 2020, Torres-Montilla and Rodriguez-Concepcion 2021), while osmiophilic PGs of chloroplasts contain only trace amounts of carotenoids (Lichtenthaler 2007). Until September 24 the content of $\beta\text{-Car}$ was comparable to summer values, despite its consumption in the biosynthesis of derivatives: Rhd and Vx. It can be assumed that in this period there is an increase in the *de novo* biosynthesis of $\beta\text{-Car}$, which is associated with the buildup of its metabolism outside the thylakoids, leading to the appearance of Rhd, and the biosynthesis of additional amounts of Vx (Fig. 2). A pronounced decrease in the content of $\beta\text{-Car}$ was observed in the temperature range from near zero to -8°C (Table 2) with a simultaneous sharp increase in the Rhd content (Fig. 2A). Obviously, a part of the $\beta\text{-Car}$ was involved in Rhd biosynthesis during the progression of chloroplast-to-chromoplast transformation (Merzlyak *et al.* 2005). The multistep conversion of $\beta\text{-Car}$ to Rhd includes intermediates such as $\beta\text{-cryptoxanthin}$ and Zx (Royer *et al.* 2020). The appearance of Rhd indicates the induction of a photoprotective mechanism based on optical screening (Merzlyak *et al.* 2005) under low temperatures before the establishment of snow cover in autumn and the resumption of active photosynthesis after

the snow cover melts. It should be noted that in Central Yakutia, snow completely melts at the end of April, while photosynthesis in ephedra resumes at the end of May. In the absence of photosynthesis, ephedra plants are subjected to a combination of high insolation (average daily PAR from 380 to 750 with a maximum of 900 to 1 100 $\mu\text{mol}(\text{photon})\text{ m}^{-2}\text{ s}^{-1}$) and low average daily temperatures of +4 - +8°C in the first half of May.

Unlike most evergreen conifers (Verhoeven 2014), the Vx cycle pigments content in January was comparable to summer values as a result of a sharp drop in Vx content in the range of average daily temperatures from +6 to -5°C (Fig. 2B). We assume that in addition to an operation of the Vx cycle in which Vx is converted to Zx, this phenomenon is associated with a more extended set of metabolic pathways for Vx. Unlike neoxanthin (data not shown), the fall in Vx by September 24 was more pronounced compared to the fall in Chls (Fig. 2B) and consequently in Chl-binding antenna proteins. According to the results, it can be assumed that during chloroplast rearrangement, including degradation of thylakoids and accumulation of PGs, part of Vx eventually is cleaved (Rottet et al. 2016).

The appearance of Zx fraction unregulated by light was observed at the onset of negative temperatures at night and early morning (end of September). Its accumulation continued during October upon freezing temperatures (Table 2) and concomitant exposure to the average daylight irradiance from 150 to 460 $\mu\text{mol}(\text{photon})\text{ m}^{-2}\text{ s}^{-1}$. Since this period, Zx is engaged in sustained NPQ of excess light energy with a decrease in maximal photochemical efficiency (ϕ_{P_680}) of PSII from 0.63 (September 24) to 0.56 on October 3 (Table 3). This event in evergreen plants leads to destacking of appressed grana of thylakoid membranes (Grebe et al. 2020). Apart from the role of Zx in modulating thermal dissipation of excess energy absorbed by photosynthetic apparatus (Jahns et al. 2009, Verhoeven 2014), its constitutive accumulation suggests the presence of free Zx molecules in the membrane lipid phase. In this case, free Zx molecules can act as direct antioxidants and membrane stabilizers, having a synergistic effect with α -Toc (Havaux and García-Plazaola 2014).

In photosynthetic tissues, α -Toc is found in all chloroplast membranes (thylakoids, envelopes, osmiophilic PGs connected to the thylakoid membrane) (Lichtenthaler 2007, Havaux and García-Plazaola 2014). The antioxidant activity of α -Toc results from direct chemical reaction with photosynthesis-derived ROS and prevention of the propagation of lipid peroxidation by scavenging lipid peroxyl radicals in the thylakoid membrane. Physical quenching of $^1\text{O}_2^*$ constitutes yet another important role of α -Toc in the protection of PSII reaction centers against photoinhibition (Munné-Bosch 2005, Krieger-Liszky and Trebst 2006).

In the ephedra the total content of α -Toc was found to exceed the content of other lipophilic antioxidants (β -Car, PQs, Zx) which is consistent with the data from the literature (Fernández-Marín et al. 2017). α -Toc accounted for more than 99% of total tocopherols in ephedra plants.

Such a composition is typical for coniferous evergreen plants in which the content of α -Toc is lower than in the case of deciduous trees (Szymańska and Kruk 2008, Strzalka et al. 2009). In July, the content of α -Toc is comparable to its content in *Pinus sylvestris* and *Araucaria araucana* (Strzalka et al. 2009). In mid-August, an increase of α -Toc by 17% was observed due to a change in the phenology of the shoots (Table 2). The accumulation of α -Toc in tree leaves during their growth and development is well known (Szymańska and Kruk 2008).

The seasonal decrease in average daily temperatures led to a further gradual increase in the content of α -Toc by about 20% compared to August (Table 2). Maximum values of α -Toc were detected on October 7. On October 4 and 5 in the absence of snow cover, the plants were subjected to temperatures -2.7 ± 2.9 (day) and -6.3 ± 1.8 °C (night). Since α -Toc is the main scavenger of $^1\text{O}_2^*$ and lipid peroxyl radicals, the increase in this antioxidant is reasonable. In contrast to evergreen Mediterranean broadleaf trees and shrubs (García-Plazaola et al. 2003), the low modifications in content of α -Toc in response to a severe period of freezing temperatures distinguish *E. monosperma*. Early dramatic reduction in PSII photochemical efficiency (Table 3) and the synthesis of Rhd from β -Car prevent the need for a pronounced increase in α -Toc. A similar pattern was observed in evergreen *Buxus sempervirens* that accumulate the red (*retro*) carotenoids eschscholtzanthin and its derivatives in winter (García-Plazaola et al. 2003, Hormaetxe et al. 2005).

The PQ pool carries electrons in the linear and alternative electron transport such as the chlororespiratory pathway and cyclic electron flows around PSI and PSII (Havaux 2020). The main form of PQ in plants is PQ-9, which contains a nonaprenyl side chain. PQ-9 located in thylakoid membranes also has potent antioxidant activity: it is capable of scavenging ROS produced during photosynthesis (Szymańska and Kruk 2010, Strzalka et al. 2011, Havaux 2020) and mitigates lipid peroxidation (Nowicka et al. 2013). Antioxidant activity is also provided by the phenolic group of reduced PQ-9 (beside a nonaprenyl side chain). The reduced PQ-9 is likely to be a better $^1\text{O}_2^*$ scavenger than oxidized PQ-9. It should be noted that the fraction (up to 50%) of the PQ pool located in the PGs and the chloroplast envelopes is photochemically nonactive (Havaux 2020, Ksas et al. 2022).

To examine whether the increase in the PQ content (Fig. 3B) is related to the photochemically active PQ pool or to the photochemically non-active PQ pool, which is mainly localized in PGs, we assessed the seasonal dynamic of photochemically active PQ fraction using the OJIP curves (Fig. 4).

The OJIP curves measured in July, August, and in the beginning of September comprised three clearly visible kinetic stages (Fig. 4) representing the light-induced reduction of the following pools: the PSII acceptor side (OJ phase), the plastoquinone pool (JI), and the entire photosynthetic electron-transport chain (ETC), including PSI (IP) (Antal and Rubín 2008). F_0 decreased with the decrease in temperature. This is consistent with a gradual

decrease in Chl *a* content in *Ephedra* shoots from 2.7 to 1.6 mg g⁻¹(DM) during the study period.

A gradual increase in the amplitude of relative variable fluorescence in the OJ phase (the parameter V_i) during the seasonal decrease in air temperature (Table 3) can be attributed to an accumulation of Q_A⁻ in PSII RCs after the slowdown of electron transport beyond Q_A (Chen *et al.* 2014). While the relative amplitude of the JIP transition (or the parameter Ψ_o) is a measure of the ability of PSII to reduce the plastoquinone pool (Strasser *et al.* 2004). The highest amplitude of the JIP transition was observed from July to early September, and then it decreased steadily from late September to December (Fig. 4, Table 3). This is corroborated by the electron transport-related parameter φ_{Eo}, which decreased significantly from September 9 until October 3. The parameters F_m and φ_{Po} dropped dramatically (Table 3, Fig. 4) at the end of September and beginning of October, when temperatures dropped from 4 to -1.5°C (Fig. 1). As the density of active PSII RCs is proportional to F_m and φ_{Po} (Chen *et al.* 2014), we suggest that the amount of active PSII RCs decreased and caused blocking of PSII electron transport at the acceptor side, and damage to pigment assemblies (F_m, Chls). Obviously, during cold acclimation in shoots of *E. monosperma*, a steady decrease in the size of the photoactive PQ pool occurs caused by a reduction in the number of active PSII complexes.

However, according to HPLC analysis data, with a seasonal decrease in temperature from 8.1°C to near zero temperatures, the content of PQH₂ increased by 2.5 times (compared to July) and PQ by 1.4 times, the content of PQ_{tot} 1.7 times (Fig. 3B). Lower positive temperatures were found to be the most effective in inducing the expression of the *VTE1* and *VTE4* genes and causing accumulation of PQ (Gabruk *et al.* 2016). A more pronounced increase in PQH₂ is due to the fact that the primary biosynthetic form of PQ is PQH₂, the reduced form. Under prolonged exposure to freezing temperatures during October - January, the content of PQH₂ gradually decreased 2.2 times. The oxidized form of PQ in PGs is probably formed non-enzymatically from PQH₂ by its oxidation with ROS. Although PQH₂/PQ were prone to oxidation at -3.2 to -7.4°C before the establishment of snow cover in late autumn, the content of PQ_{tot} (oxidized and reduced) in the winter months was 1.5 times higher than at the end of July. Obviously, the observed increase in the amounts of PQH₂/PQ (Fig. 3B) during cold hardening of *E. monosperma* plants occurs due to the accumulation of the photochemically inactive PQ_{tot} pool outside the thylakoid membranes, namely in the PGs and envelopes.

During the period of resumption of the ephedra photosynthesis in Central Yakutia at the end of May, sunny days with high insolation reaching a maximum of 900 - 1100 μmol(photon) m⁻² s⁻¹ prevailed. Mild air temperatures were recorded with a daily mean of 10 to 12°C. Low temperatures in the layer of the soil inhabited by roots, ranging from +2 to +6°C, are the main limiting factor for resumption of photosynthesis. Under such condition a consumption of the photoactive PQ pool may take place due to oxidative stress at early stages of the photosynthetic apparatus reassembly. The maintenance and progressive

increase in PQ content in the thylakoid membranes would depend on their mobilization from the non-photoactive PQ pool stored in PGs.

Our study presents a field characterization of the content of lipophilic antioxidants in ephedra plants during shortening of the photoperiod and a seasonal decrease in temperature which affects the overwintering success of these plants. We hypothesize the following outcomes: the season-long reduction in φ_{Po} (PSII efficiency) by the end of September resulted in significant decrease in photosynthetic electron transport (given as φ_{Eo}) at near zero temperatures. This may lead to sufficient frost hardiness even with a moderate increase in lipophilic antioxidants as part of acclimatory response. Further increases of their content in response to extreme sub-zero temperatures (-30 to -45°C) were not required in frozen plants overwintering under a snowpack. We suggest that a non-dramatic consumption of PQ/PQH₂, α-Toc may occur during late autumn days with mild freezing temperatures before the establishment of snow cover, as well as during spring days with warm air temperatures after snowmelt, while the soil remains cold. Probably such a seasonal pattern of lipophilic antioxidants is ecologically advantageous to the evergreen plants overwintering under snow.

Conclusions

Low temperatures during cold acclimation of the field-grown evergreen shrub *E. monosperma* led to the higher content of α-Toc, Zx, PQ/PQH₂ and decrease in the β-Car content accompanied by a sharp increase in the content of Rhd. The increase in PQ pool in autumn is due to increase in photochemically inactive PQ/PQH₂. We revealed different timing and temperature ranges of variation for individual antioxidants.

References

- Antal T., Rubin A.: *In vivo* analysis of chlorophyll *a* fluorescence induction. - *Photosynth. Res.* **96**: 217-226, 2008.
- Cazzaniga S., Li Z., Niyogi K.K. *et al.*: The *Arabidopsis szll* mutant reveals a critical role of β-carotene in photosystem I photoprotection. - *Plant Physiol.* **159**: 1745-1758, 2012.
- Chen S., Strasser R.J., Qiang S.: *In vivo* assessment of effect of phytotoxin tenuazonic acid on PSII reaction centers. - *Plant Physiol. Biochem.* **84**: 10-21, 2014.
- Fernández-Marin B., Hernández A., Garcia-Plazaola J.I. *et al.*: Photoprotective strategies of Mediterranean plants in relation to morphological traits and natural environmental pressure: a meta-analytical approach. - *Front. Plant Sci.* **8**: 1051, 2017.
- Gabruk M., Habina I., Kruk J. *et al.*: Natural variation in tocochromanols content in *Arabidopsis thaliana* accessions – the effect of temperature and light intensity. - *Physiol. Plantarum* **157**: 147-160, 2016.
- Garcia-Plazaola J.I., Olano J.M., Hernández A., Becerril J.M.: Photoprotection in evergreen Mediterranean plants during sudden periods of intense cold weather. - *Trees* **17**: 285-291, 2003.
- González-Rodríguez Á.M., Brito P., Lorenzo J.R., Jiménez M.S.:

- Photosynthetic performance in *Pinus canariensis* at semi-arid treeline: phenotype variability to cope with stressful environment. - *Forests* **10**: 845, 2019.
- Grebe S., Trottaa A., Bajwaa A.A., Aro E.-M.: Specific thylakoid protein phosphorylations are prerequisites for overwintering of Norway spruce (*Picea abies*) photosynthesis. - *PNAS* **117**: 17499-17509, 2020.
- Havaux M.: Plastoquinone in and beyond photosynthesis. - *Trends Plant Sci.* **12**: 1252-1265, 2020.
- Havaux M., García-Plazaola J.I.: Beyond non-photochemical fluorescence quenching: the overlapping antioxidant functions of zeaxanthin and tocopherols. - In: Demmig-Adams B., Garab G., Adams III W., Govindjee (ed.): *Non-Photochemical Quenching and Energy Dissipation in Plants, Algae and Cyanobacteria*. *Advances in Photosynthesis and Respiration*. Vol. 40. Pp. 583-603. Springer, Dordrecht 2014.
- Hormaetxe K., Becerril J.M., Fleck I. *et al.*: Functional role of red (*retro*)-carotenoids as passive light filters in the leaves of *Buxus sempervirens* L.: increased protection of photosynthetic tissues? - *J. Exp. Bot.* **56**: 2629-2636, 2005.
- Jahns P., Latowski D., Strzalka K.: Mechanism and regulation of the violaxanthin cycle: the role of antenna proteins and membrane lipids. - *BBA-Bioenergetics* **1787**: 3-14, 2009.
- Katahata S.-I., Katoh M., Iio A., Mukai Y.: Photoinhibition and pigment composition in relation to needle reddening in sun-exposed *Cryptomeria japonica* at different altitudes in winter. - *J. For. Res.-Jpn.* **27**: 148-157, 2021.
- Krieger-Liszczak A., Trebst A.: Tocopherol is the scavenger of singlet oxygen produced by the triplet states of chlorophyll in the PSII reaction centre. - *J. Exp. Bot.* **57**: 1677-1684, 2006.
- Kruk J., Trebst A.: Plastoquinol as a singlet oxygen scavenger in photosystem II. - *BBA-Bioenergetics* **1777**: 154-162, 2008.
- Ksas B., Alric J., Caffarri S., Havaux M.: Plastoquinone homeostasis in plant acclimation to light intensity. - *Photosynth. Res.* **152**: 43-54, 2022.
- Kuczynska P., Jemiola-Rzeminska M.: Isolation and purification of all-*trans* diadinoxanthin and all-*trans* diatoxanthin from diatom *Phaeodactylum tricoratum*. - *J. Appl. Phycol.* **29**: 79-87, 2017.
- Lichtenthaler H.K.: Chlorophylls and carotenoids: pigments of photosynthetic biomembranes. - *Method. Enzymol.* **148**: 350-382, 1987.
- Lichtenthaler H.K.: Biosynthesis, accumulation and emission of carotenoids, α -tocopherol, plastoquinone, and isoprene in leaves under high photosynthetic irradiance. - *Photosynth. Res.* **92**: 163-179, 2007.
- Maslova T.G., Mamushina N.S., Sherstneva O.A. *et al.*: Seasonal structural and functional changes in the photosynthetic apparatus of evergreen conifers. - *Russ. J. Plant Physiol.* **56**: 607-615, 2009.
- Merzlyak M., Solovchenko A., Pogosyan S.: Optical properties of rhodoxanthin accumulated in *Aloe arborescens* Mill. leaves under high-light stress with special reference to its photoprotective function. - *Photoch. Photobio. Sci.* **4**: 333-340, 2005.
- Munné-Bosch S.: The role of α -tocopherol in plant stress tolerance. - *J. Plant Physiol.* **162**: 743-748, 2005.
- Nowicka B., Gruszka J., Kruk J.: Function of plastoquinone and other biological prenyllipids in the inhibition of lipid peroxidation – A comparative study in model systems. - *BBA-Biomembranes* **1828**: 233-240, 2013.
- Nowicka B., Kruk J.: Plastoquinol is more active than α -tocopherol in singlet oxygen scavenging during high light stress of *Chlamydomonas reinhardtii*. - *BBA-Bioenergetics* **1817**: 389-394, 2012.
- Rottet S., Devillers J., Glauser G. *et al.*: Identification of plastoglobules as a site of carotenoid cleavage. - *Front. Plant Sci.* **7**: 1855, 2016.
- Royer J., Shanklin J., Balch-Kenney N. *et al.*: Rhodoxanthin synthase from honeysuckle; a membrane diiron enzyme catalyzes the multistep conversion of β -carotene to rhodoxanthin. - *Sci. Adv.* **6**: eaay9226, 2020.
- Sofronova V.E., Chepalov V.A., Dymova O.V., Golovko T.K.: The role of pigment system of an evergreen dwarf shrub *Ephedra monosperma* in adaptation to the climate of Central Yakutia. - *Russ. J. Plant Physiol.* **61**: 246-254, 2014.
- Strasser R.J., Tsimilli-Michael M., Srivastava A.: Analysis of the chlorophyll *a* fluorescence transient. - In: Papageorgiou G.C., Govindjee (ed.): *Chlorophyll *a* Fluorescence: A Signature of Photosynthesis*. *Advances in Photosynthesis and Respiration*. Vol. 19. Pp. 321-362. Springer, Dordrecht 2004.
- Strzalka K., Szymanska R., Suwalsky M.: Prenylipids and pigments content in selected antarctic lichens and mosses. - *J. Chil. Chem. Soc.* **56**: 808-811, 2011.
- Strzalka K., Szymanska R., Swiezewska E. *et al.*: Tocochromanols, plastoquinone and polyprenols in selected plant species from Chilean Patagonia. - *Acta Biol. Cracov. Bot.* **51**: 39-44, 2009.
- Szymańska R., Kruk J.: Plastoquinol is the main prenyllipid synthesized during acclimation to high light conditions in *Arabidopsis* and is converted to plastoquinone by tocopherol cyclase. - *Plant Cell Physiol.* **51**: 537-545, 2010.
- Szymańska R., Kruk J.: Tocopherol content and isomers' composition in selected plant species. - *Plant Physiol. Biochem.* **46**: 29-33, 2008.
- Torres-Montilla S., Rodriguez-Concepcion M.: Making extra room for carotenoids in plant cells: new opportunities for biofortification. - *Prog. Lipid Res.* **84**: 101128, 2021.
- Verhoeven A.: Sustained energy dissipation in winter evergreens. - *New Phytol.* **201**: 57-65, 2014.
- Zhirkov A., Permyakov P., Wen Z., Kirillin A.: Influence of rainfall changes on the temperature regime of permafrost in Central Yakutia. - *Land* **10**: 1230, 2021.